World Journal of Advanced Research and Reviews
eISSN: 2581-9615 CODEN (USA): WJARAI
Cross Ref DOI: 10.30574/wjarr
Journal homepage: https://wjarr.com/

(RESEARCH ARTICLE)

Check for updates

Synthesis and biological evaluation of cyclohexanpyridin-2(1*H*)-one analogues as novel HIV-1 NNRTIs

Gibrán Rodríguez-Vega [1, 2, #], Julio Cesar Abarca-Magaña [3, #], Nancy Vanessa Castro-Perea [1], Mirna Berenice Ruiz-Rivera [3], José Luis Medina-Franco [4], Leonor Huerta-Hernández [3] and Daniel Chávez [1,*]

[1] *National Technological of Mexico /Tijuana Technological Institute, Center for Graduate and Research in Chemistry, Postal Box 1166, Tijuana, Baja California 22000, Mexico.*
[2] *Academic Unit of Chemical Biological and Pharmaceutical Sciences, Autonomous University of Nayarit, Tepic, Nayarit 63000, Mexico.*
[3] *Biomedical Research Institute, Department of Immunology,National Autonomous University of Mexico, Mexico City 04510, Mexico.*
[4] *DIFACQUIM Research group, Department of Pharmacy, School of Chemistry, National Autonomous University of Mexico, Mexico City 04510, Mexico.*
[#] *Authors contributed equally to this work.*

World Journal of Advanced Research and Reviews, 2024, 22(03), 369–385

Publication history: Received on 24 April 2024 revised on 01 June 2024; accepted on 03 June 2024

Article DOI: https://doi.org/10.30574/wjarr.2024.22.3.1684

Abstract

In the search and development of new non-nucleoside reverse transcriptase inhibitor (NNRTI) compounds that are more effective against HIV-1, eight C-4 alkylated cyclohexanpyridinone derivatives of the alkyloxy and alkylamino type were synthesized. Compounds were characterized by spectroscopic and spectrometric techniques. In addition, their inhibitory effect against reverse transcriptase (RT), inhibition of HIV *in vitro* and cytotoxicity in JLTRG cells was evaluated. Compound *8e* showed reasonable cellular antiviral activity (EC_{50} = 28.78 μM), moderate inhibition against RT (IC_{50} = 69.8 μM), and was not cytotoxic at the concentrations evaluated. Docking and molecular dynamics studies corroborate favorable binding to the HIV IT allosteric site with *8e*, providing a basis for the design of more potent analogues.

Keywords: HIV-1; NNRTI; Reverse transcriptase; Pyridinones; Docking; Cytotoxicity; HIV infectivity; Molecular dynamics

1. Introduction

The Human Immunodeficiency Virus (HIV) is the causative agent of the Acquired Immunodeficiency Syndrome (AIDS) pandemic. According to UNAIDS data, there were 39 million people around the world living with HIV in 2022 [1]. Currently, a notable reduction in AIDS-related mortality has been made possible by highly active antiretroviral therapy (HAART). HAART targets multiple cycles of viral replication and includes two nucleoside reverse transcriptase inhibitors (NRTIs), a non-nucleoside reverse transcriptase inhibitor (NNRTIs), and a protease inhibitor (PI) or integrase inhibitor (INSTI) [2, 3]. One of the biggest challenges of HAART is that the virus can acquire drug resistance mutations, resistance arises as a result of poor patient adherence, allowing viral replication and mutation [4].

The development of specific inhibitors against the replication of HIV to reduce viral infection continues to be a leading treatment strategy against HIV [5, 6]. NNRTIs such as nevirapine and efavirenz (Figure 1) have been positioned as

* Corresponding author: Daniel Chávez

essential components in therapies combinations of drugs due to their unique antiviral activity, high specificity, and low toxicity [6, 7, 8].

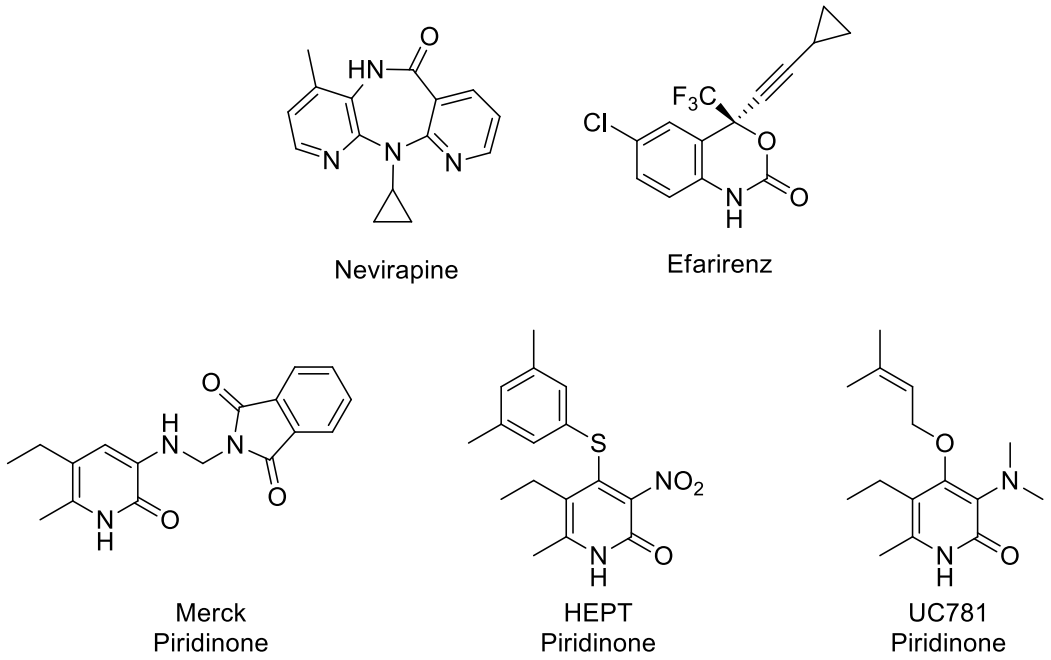

Figure 1 Chemical structures of approved NNRTIs (nevirapine and efavirenz) and pyridinone hybrids.

A promising group of NNRTIs that has aroused the interest of researchers in recent years is that of compounds based on the pyridinone nucleus [9]. Merck's pyridinone (Figure 1) was the first potent and selective reverse transcriptase inhibitor of HIV-1 described from this group [10]. Using Merck's pyridinone nucleus, so-called first-generation compounds were developed, such as the pyridinone-HEPT hybrid, to which, however, HIV showed resistance. Rigidity is not desirable for NNRTIs, as they become ineffective due to most mutations, especially Y181C, Y188L and K103N [11, 12, 13]. Some internal flexibility and small size have been reported to be desirable to allow NNRTIs to be adjust to mutations; a perfect fit for wild type reverse transcriptase with a rigid inhibitor is not desirable [11, 12, 13].

A series of second-generation hybrids were synthesized to optimize Merck pyridinones against resistant strains, such as the hybrids pyridinone-HEPT, and pyridinone UC781 (Figure 1) [9]. Unlike introducing a substituent with an aromatic ring at C-4 as in HEPT-pyridinones, the strategy of including an aliphatic substituent at the same C-4 position was proposed in hybrids and pyridinone derivatives as UC781 [9]. The aliphatic substituent be intendent to perform interactions with conserved residues such as W229 and aromatic π–π interactions with Y181,–although such interactions should be less significant compared to the aromatic π–π interactions of the original Merck pyridinones [14].

Here in, we report the design, synthesis, biological evaluation, docking and molecular dynamics (MD) of eight cyclohexanpyridinone derivatives as novel HIV-1 NNRTIs. The antiviral activities of all compounds were tested in HIV-1IIIB-infected JLTRG reporter cells and structure-activity relationships were established. We profiled the drug-like properties of the newly designed compounds and performed docking studies to gain insights into the binding modes of representative compounds and understand the biological potencies.

2. Material and methods

2.1. General Procedures

^{1}H and ^{13}C NMR spectra of all compounds were collected on a Bruker Avance III spectrometer (400 MHz) and are expressed in ppm using TMS as an internal standard. The solvents used were $CDCl_3$ and DMSO. Electron impact ionization (EMIE) mass spectra were acquired on an Agilent Technologies 5975C. Functional group analysis by infrared (IR) spectroscopy was performed on a Fourier Spectrum 400 FT-IR infrared spectrophotometer, Pekin Elmer. The melting points were determined in a Fisher-Johns series 4114 apparatus. The percentage of fluorescent cells expressing the EGFP protein was measured by flow cytometry using the Attune Blue/Violet cytometer (Thermo Fisher, USA).

Fluorescence measurement for activity against RT was performed on a BioTek spectrophotometer, USA, cell viability data were acquired on an iMark Bio Rad microplate reader.

2.2. Synthesis of cyclohexanpyridin-2(1*H*)-one analogues

2.2.1. Ethyl 2-aminocyclohex-1-enecarboxylate (2)

Ethyl 2-oxocyclohexanecarboxylate *(1)* (25 g, 146.98 mmol) and ammonium nitrate (12.94 g, 161.67 mmol) were added in 150 mL of THF. The mixture was stirred for 5 d with bubbling ammonia for 30 min eight times a day. After this time, the solvent was removed, subsequently 150 mL of water was added, and the mixture was stirred for 30 min. The colorless residue was filtered and recrystallized in hexane to obtain compound *2* as a white solid. (24.34 g, 98%). Mp. 61 °C. IR (KBr): 3427, 3321, 2978, 2930, 2840, 1649, 1607, 1531 cm^{-1}. ^1H NMR ($CDCl_3$, 400 MHz) δ 6.00 (bs, $N\underline{H}_2$), 4.14 (q, *J*=7.1 Hz, $COOC\underline{H}_2CH_3$), 2.25 (t, *J*=5.6 Hz, 2H, H-6), 2.20 (t, *J*=6.0 Hz, 2H, H-3), 1.60 (m, 4H, H-4 y H-5), 1.27 (t, *J*=7.1 Hz, $COOCH_2C\underline{H}_3$). ^{13}C NMR ($CDCl_3$, 100 MHz) δ 170.4, 156.4, 92.3, 58.8, 30.6, 23.4, 23.1, 22.2, 14.6. EIMS *m/z* (Rel. Ab): M^+ 169 (80), 140 (90), 124 (60), 96 (100).

2.2.2. Ethyl 4-hydroxy-2-oxo-1,2,5,6,7,8-hexahydroquinoline-3-carboxylate (3)

Metallic sodium (1.36 g, 59.14 mmol) was slowly dissolved in 20 mL of ethanol under nitrogen atmosphere. The mixture was heated to reflux and diethyl malonate (9 mL, 59.14 mmol) was added dropwise for 30 min under reflux. Compound *2* (5 g, 29.57 mmol) dissolved in ethanol was added dropwise for 30 min. The mixture was stirred with reflux for 72 h to obtain a pale-yellow solution, which was cooled to room temperature and the precipitate filtered. The solid was dissolved in ice water and acidified to pH 1 with a solution of concentrated solution of hydrochloric acid. The precipitate was filtered, washed with water and recrystallized with ethyl ether to obtain compound *3* as a white solid (6.0 g, 85%). Mp 205 °C. IR (KBr): 3336, 3164, 3053, 2982, 2940, 2749, 1656, 1628, 1567 cm^{-1}. ^1H NMR ($DMSO$, 400 MHz) δ 13.45 (s, O<u>H</u>), 11.15 (s, N<u>H</u>), 4.30 (q, *J* = 7.1 Hz, $COOC\underline{H}_2CH_3$), 2.50 (t, *J* = 5.4, 2H, H-8), 2.30 (t, *J* = 5.3 Hz, 2H, H-5), 1.60 (m, 4H, H-6 y H-7), 1.30 (t, *J* = 7.1 Hz, $COOCH_2C\underline{H}_3$). ^{13}C NMR ($CDCl_3$, 100 MHz) δ 173.8, 172.5, 159.7, 150.9, 105.1, 96.4, 61.3, 26.9, 21.7, 21.3, 20.5, 14.6. EIMS *m/z* (Rel. Ab): $[M]^+$ 237 (40), 191 (45), 163 (75), 135 (100).

2.2.3. Ethyl 2-(benzyloxy)-4-hydroxy-5,6,7,8-tetrahydroquinoline-3-carboxylate (4)

Compound *3* (5 g, 21.1 mmol) and silver carbonate (3.32 g, 12.03 mmol) were dissolved in 100 mL of THF; benzyl bromide in 20 mL of THF (3.59 g, 21.1 mmol) was added dropwise; the mixture was heated to reflux under nitrogen atmosphere for 8 h. The mixture was cooled to room temperature. The organic solution was then extracted with dichloromethane and then concentrated under reduced pressure to obtain compound *4* as a white solid (4 g, 58%). Mp 60 °C. IR (KBr): 3372, 2987, 2939, 2815, 1646, 1623 cm^{-1}. ^1H NMR ($CDCl_3$, 400 MHz) δ 12.60 (br. s, O<u>H</u>), 7.50-7.29 (m, 5H), 5.40 (s, $C\underline{H}_2$-Ar), 4.38 (q, *J* = 7.2 Hz, $COOC\underline{H}_2CH_3$), 2.71 (t, *J* = 6.0 Hz, 2H, H-8), 2.57 (t, *J* = 6.4 Hz, 2H, H-5), 1.79 (m, 4H, H-6 y H-7), 1.34 (t, *J* = 7.2 Hz, $COOCH_2C\underline{H}_3$). ^{13}C NMR ($CDCl_3$, 100 MHz) δ 171.5, 169.2, 160.1, 159.5, 137.7, 128.1, 127.5, 127.4, 114.6, 94.6, 67.8, 61.6, 32.9, 22.6, 22.1, 21.6, 14.0. EIMS *m/z* (Rel. Ab): $[M]^+$ 327 (45), 149 (85), 91 (100).

2.2.4. (E)-ethyl 2-(benzyloxy)-4-(but-2-en-1-yloxy)-5,6,7,8-tetrahydroquinoline-3-carboxylate (5a)

In a round bottom flask were added compound *4* (3.0 g, 9.17 mmol) and potassium carbonate (2.53 g, 18.35 mmol) in DMF. Crotyl bromide (2.48 g, 18.35 mmol) dissolved in ethanol was added dropwise and the mixture was stirred at reflux under an inert nitrogen atmosphere for 48 h. The mixture was cooled to room temperature, filtered to remove salt and washed with acetone. The wash and filtrate were combined and evaporated to dryness. The residue was purified by silica gel column chromatography (dichloromethane/hexane, 9:1) to obtain an amber-yellow viscous liquid (2.97 g, 85%). IR, 3058, 3027, 2928, 1726, 1645 cm^{-1}. ^1H NMR ($CDCl_3$, 400 MHz) δ 7.41-7.25 (m, 5H), 5.80 (m, CH=C<u>H</u>-CH_3), 5.67 (m, C<u>H</u>=CH-CH_3), 5.38 (s, $C\underline{H}_2$-Ar), 4.44 (ddq, *J* = 6.2, 1.1, 1.1 Hz, $C\underline{H}_2$- CH=CH-CH_3), 4.34 (q, *J* = 6.8 Hz, $COOC\underline{H}_2CH_3$), 2.74 (t, *J* = 6.4 Hz, 2H, H-8), 2.59 (t, *J* = 6.4 Hz, 2H, H-5), 1.77 (m, 4H, H-6 y H-7), 1.73 (ddt, *J* = 6.4, 1.4, 1.1 Hz, CH_2-CH=CH-$C\underline{H}_3$), 1.30 (t, *J* = 7.2 Hz, $COOCH_2C\underline{H}_3$).^{13}C NMR ($CDCl_3$, 100 MHz) δ 166.2, 162.9, 158.6, 156.8, 137.7, 130.9, 128.2, 127.5, 127.4, 126.0, 118.7, 107.2, 73.6, 67.4, 61.4, 32.5, 22.8, 22.7, 22.4, 17.8, 14.1. EIMS *m/z* (Rel. Ab): $[M]^+$ 381 (14), 281 (16), 192 (21), 149 (38) 91 (100) uma.

2.2.5. Ethyl (E)-4-(but-2-en-1-yloxy)-2-oxo-1,2,5,6,7,8-hexahydroquinoline-3-carbo- xylate (6a)

In a round bottom flask, the protected cyclohexanpyridinone-crotyloxy hybrid *5a* (1 g, 2.62 mmol) was placed in 100 mL of 1 N hydrochloric acid. It was left stirring, heating at 80 °C for 48 h; 5% sodium hydroxide was added until the solution was neutralized. A white precipitate formed, which was filtered, washed with acetone (0.38 g, 87%). ^1H NMR ($CDCl_3$, 400 MHz) δ 5.72 (m, CH=CH-CH_3), 5.55 (m, CH=CH-CH_3), 4.41 (ddq, *J* = 6.2, 1.1, 1.1 Hz, CH_2- CH=CH-CH_3), 4.35 (q, *J*=6.8 Hz, $COOCH_2CH_3$), 2.74 (t, *J*=6.5 Hz, 2H, H-8), 2.57 (t, *J*=6.5 Hz, 2H, H-5), 1.73 (m, 4H, H-6 y H-7), 1.80 (ddt, *J*=6.2,

1.1, 1.1 Hz, CH_2-CH=CH-CH_3), 1.29 (t, J=7.2 Hz, $COOCH_2CH_3$). RMN ^{13}C ($CDCl_3$, 100 MHz) δ 168.2, 163.9, 158.6, 156.2, 135.7, 125.0, 118.5, 107.2, 67.8, 61.4, 32.6, 22.7, 22.5, 22.3, 17.8, 14.4. EIMS *m/z* (Rel. Ab): $[M]^+$ 291 (12), 271 (62) 245 (16), 237 (21), 177 (38) 135 (100) uma.

2.2.6. Ethyl 2-(benzyloxy)-4-((3-methylbut-2-en-1-yl)oxy)-5,6,7,8-tetrahydroquinoline -3-carboxylate (5b)

In a round bottom flask were added compound *4* (0.3 g, 0.92 mmol) and potassium carbonate (0.25 g, 1.84 mmol) in DMF. Dimethylallyl bromide (0.27 g, 1.84 mmol) dissolved in DMF was added dropwise and the mixture was stirred at room temperature for 72 h. Later on, water (20 mL) was added and the aqueous layer was extracted with DCM (3 x 20 mL), the solvents were eliminated under vacuum to obtain compound *5b* as a viscous yellow liquid (0.235 g, 65%). IR: 2972, 2934, 2860, 1725, 1666, 1574, 1099 cm^{-1}. ^1H NMR ($CDCl_3$, 400 MHz) δ 7.42-7.24 (m, 5H), 5.45 (t*p*q, 7.2 Hz, 1.3 Hz C<u>H</u>=C-[CH_3]$_2$), 5.38 (s, C<u>H</u>$_2$-Ar), 4.51 (d, 7.2 Hz, C<u>H</u>$_2$-CH=C-[CH_3]$_2$), 4.34 (q, *J* = 7.2 Hz, COOC<u>H</u>$_2$$CH_3$), 2.74 (t, *J* = 6.4 Hz, 2H, H-8), 2.60 (t, *J* = 6.4 Hz, 2H, H-5), 1.80 (m, 4H, H-6 y H-7), 1.76 (bs, CH_2-CH=C-[C<u>H</u>$_3$]$_2$), 1.67 (bs, CH_2-CH=C-[C<u>H</u>$_3$]$_2$), 1.30 (t, *J* = 7.2 Hz, $COOCH_2$C<u>H</u>$_3$). ^{13}C NMR ($CDCl_3$, 100 MHz) δ 166.2, 163.0, 158.6, 156.7, 138.5, 137.7, 128.1, 127.4, 119.6, 118.7, 107.1, 69.6, 67.4, 61.3, 32.5, 25.7, 22.7, 22.6, 22.4, 18.0, 14.1. EIMS *m/z* (Rel. Ab): $[M]^+$ 395 (3), 350 (9), 327 (71), 281 (34), 250 (23), 192 (26), 149 (76) 91 (100) uma.

2.2.7. Ethyl 4-((3-methylbut-2-en-1-yl)oxy)-2-oxo-1,2,5,6,7,8-hexahydroquino- line-3-carboxylate (6b)

A solution of the compound *5b* (0.15 g, 0.41 mmol) in 2N HCl (20 mL) was heated to reflux for 2 d. When the reaction was completed, the mixture was extracted with DCM (3 X 20 mL). The solvent was eliminated under vacuum to obtain compound *10*. ^1H RMN ($CDCl_3$, 400 MHz) δ 5.41 (m, C<u>H</u>=C-[CH_3]$_2$), 4.56 (d, *J* = 6.8 Hz, C<u>H</u>$_2$-CH=C-[CH_3]$_2$), 4.37 (q, *J* = 7.2 COOC<u>H</u>$_2$$CH_3$), 2.59 (t, *J* = 6.0 Hz, 2H, H-8), 2.41 (t, *J* = 6.0 Hz, 2H, H-5), 1.70 (m, 4H, H-6 y H-7), 1.73 (bs, CH_2-CH=C-[C<u>H</u>$_3$]$_2$), 1.65 (bs, CH_2-CH=C-[C<u>H</u>$_3$]$_2$), 1.37 (t, *J* = 7.2 Hz, $COOCH_2$C<u>H</u>$_3$). ^{13}C RMN ($CDCl_3$, 100 MHz) δ 166.5, 165.6, 162.9 y 148.6, 144.5, 139.1, 119.1, 110.1, 68.7, 61.4, 29.6, 25.7, 22.1, 21.5, 21.4, 18.1, 14.1. EMIS *m/z* (Rel. Ab.): $[M]^+$ 305 (38), 285 (19), 259 (21), 191 (67), 163 (74), 149 (100) uma.

2.2.8. Ethyl 2-(benzyloxy)-4-((4-methylpent-3-en-1-yl)oxy)-5,6,7,8-tetrahydroquino-line-3-carboxylate (5c)

In a round bottom flask were added compound *4* (0.3 g, 0.92 mmol) and potassium carbonate (0.25 g, 1.84 mmol) in DMF. Isohexenyl bromide (0.27 g, 1.84 mmol) dissolved in DMF was added dropwise and the mixture was stirred at room temperature for 72 h. Later on, water (20 mL) was added and the aqueous layer was extracted with DCM (3 x 20 mL), the solvents were eliminated under vacuum to obtain compound *5c* as a viscous yellow liquid (0.37 g, 80%). ^1H NMR ($CDCl_3$, 400 MHz) δ 7.45-7.24 (m, 5H), 5.38 (s, C<u>H</u>$_2$-Ar), 5.14 (m, C<u>H</u>=C-[CH_3]$_2$), 4.33 (q, *J* = 7.2 Hz, COOC<u>H</u>$_2$$CH_3$), 3.97 (t, *J* = 6.8 Hz, C<u>H</u>$_2$-CH_2-CH=C-[CH_3]$_2$), 2.73 (t, *J* = 6.4 Hz, 2H, H-8), 2.57 (t, *J* = 6.4 Hz, 2H, H-5), 2.42 (dt, *J* = 7.2 Hz, 6.8 Hz, CH_2-C<u>H</u>$_2$-CH=C-[CH_3]$_2$), 1.79 (m, 4H, H-6 y H-7), 1.70 (br, CH_2-CH=C-[C<u>H</u>$_3$]$_2$), 1.63 (bs, CH_2-CH=C-[C<u>H</u>$_3$]$_2$), 1.30 (t, *J* = 7.2 Hz, $COOCH_2$C<u>H</u>$_3$). ^{13}C NMR ($CDCl_3$, 100 MHz) δ 166.4, 162.8, 158.6, 156.6, 137.8, 134.5, 128.2, 127.5, 119.4, 118.3, 106.5, 72.2, 67.4, 61.4, 32.5, 29.1 25.7, 22.8, 22.6, 22.5, 17.8, 14.1. EIMS *m/z* (Rel. Ab): $[M]^+$ 409 (41), 364 (14), 327 (75), 281 (47), 250 (36), 192 (45), 149 (60) 91 (100) uma.

2.2.9. Ethyl 4-((4-methylpent-3-en-1-yl)oxy)-2-oxo-1,2,5,6,7,8-hexahydroquino- line-3-carboxylate (6c)

A solution of the compound *5c* (0.1 g, 0.24 mmol) in 2N HCl (20 mL) was heated to reflux for 2 d. When the reaction was completed, the mixture was extracted with DCM (3 X 20 mL). The solvent was eliminated under vacuum to obtain compound *6c*. ^1H RMN ($CDCl_3$, 400 MHz) δ 5.11 (m, C<u>H</u>=C-[CH_3]$_2$), 4.36 (q, *J* = 7.2 Hz, COOC<u>H</u>$_2$$CH_3$), 4.03 (t, *J* = 6.8 Hz, C<u>H</u>$_2$-CH_2-CH=C-[CH_3]$_2$), 2.60 (t, 2H, H-8), 2.40 (t, 2H, H-5), 2.30 (dt, CH_2-C<u>H</u>$_2$-CH=C-[CH_3]$_2$), 1.79 (m, 4H, H-6 y H-7), 1.70 (bs, CH_2-CH=C-[C<u>H</u>$_3$]$_2$), 1.63 (bs, CH_2-CH=C-[C<u>H</u>$_3$]$_2$), 1.36 (t, *J* = 7.2 Hz, $COOCH_2$C<u>H</u>$_3$). EIMS *m/z* (Rel. Ab): $[M]^+$ 319 (20), 280 (6), 246 (27), 238 (32), 192 (100) 165 (86), 135 (45) uma.

2.2.10. 2-(benzyloxy)-4-(cyanomethoxy)-5,6,7,8-tetrahydroquinoline-3-carboxylate (5d)

Compound *4* (0.15 g, 0.46 mmol) and potassium carbonate (0.127 g, 0.92 mmol) were dissolved in DMF (20 mL). 2-bromoacetonitrile (2.96 g, 24.46 mmol) dissolved in DMF was added dropwise and the mixture was stirred at room temperature for 24 h. Later on, water (20 mL) was added and the aqueous layer was extracted with DCM (2 x 30 mL), the solvents were eliminated under vacuum to obtain compound *5d* as a viscous brown liquid (0.14 g, 83%). IR: 3058, 2939, 2860, 1717, 1671, 1594, 1430, 1130 cm^{-1}. ^1H NMR ($CDCl_3$, 400 MHz) δ 7.42-7.26 (m, 5H), 5.39 (s, C<u>H</u>$_2$-Ar), 4.78 (s, C<u>H</u>$_2$-CN), 4.36 (q, *J* = 7.2 Hz, COOC<u>H</u>$_2$$CH_3$), 2.78 (t, *J* = 6.0 Hz, 2H, H-8), 2.68 (t, *J* = 6.0 Hz, 2H, H-5), 1.80 (m, 4H, H-6 y H-7), 1.31 (t, *J* = 7.2 Hz, $COOCH_2$C<u>H</u>$_3$). ^{13}C NMR ($CDCl_3$, 100 MHz) δ 165.1, 161.6, 158.9, 158.8, 137.3, 128.3, 127.6, 118.9, 115.0, 108.1, 67.9, 61.9, 58.3, 32.6, 22.5, 22.4, 22.1, 14.1. EIMS *m/z* (Rel. Ab.): $[M]^+$ 366 (22), 326 (18), 280 (38), 212 (69), 91 (100) uma.

2.2.11. Ethyl 4-(cyanomethoxy)-2-oxo-1,2,5,6,7,8-hexahydroquinoline-3-carboxylate (6d)

A solution of the compound *5d* (0.1 g, 0.27 mmol) in 2N HCl (20 mL) was heated to reflux for 2 d. When the reaction was completed, the mixture was extracted with DCM (3 X 20 mL). The solvent was eliminated under vacuum to obtain compound *6d*. ^{1}H RMN ($CDCl_3$, 400 MHz) δ 5.00 (s, $C\underline{H}_2$-CN), 4.42 (q, $COOC\underline{H}_2CH_3$), 2.82 (t, 2H, H-8), 2.71 (t, 2H, H-5), 1.81 (m, 4H, H-6 y H-7), 1.39 (t, $COOCH_2C\underline{H}_3$). EIMS *m/z* (Rel. Ab): $[M]^+$ 276 (15), 270 (30), 247 (43), 229 (73), 73 (100) uma.

2.2.12. 4-chloro-5,6,7,8-tetrahydroquinolin-2(1H)-one (7)

Compound *3* (0.4 g, 2.42 mmol) and benzyl trimethyl ammonium chloride (2.20 g, 9.68 mmol) were dissolved in 10 mL of *acetonitrile*; phosphoryl chloride (0.56 g, 3.63 mmol) was added dropwise. The mixture was stirred at room temperature for 24 h. Past this time, ice water was added and a white precipitated formed, which was filtered to obtain compound 7 as a white solid (92%). ^{1}H NMR ($CDCl_3$), 400 MHz): δ 4.41 (q, *J* = 7.2 Hz, $COOCH_2CH_3$), 2.66 (br, 2H, H-8), 2.53 (br, 2H, H-5), 1.78 (m, 4H, H-6 y H-7), 1.38 (t, *J* = 7.2 Hz, $COOCH_2CH_3$). RMN ^{13}C ($CDCl_3$, 100 MHz): δ 164.4, 160.6, 147.4, 146.1, 122.0, 113.8, 61.8, 27.1, 24.3, 22.2, 21.1, 14.1. EIMS *m/z* (Rel. Ab.): $[M]^+$ 255 (42), $[M]^+$+2 257 (14), 212 (19), 210 (60), 185 (27), 183 (100), 181 (51) uma.

2.2.13. Ethyl 2-oxo-4-(propylamino)-1,2,5,6,7,8-hexahydroquinoline-3-carboxylate (8e)

In a round bottom flask, compound *7* (50 mg, 0.196 mmol) and ethanol (15 mL) were added. Once stirring started, propylamine (0.064 mL, 0.784 mmol) was added drop by drop. The mixture was stirred for 48 h at reflux. Once the heating was completed, the mixture was cooled and concentrated in a rotary evaporator. Subsequently, the compound was purified by column chromatography with an ethyl acetate mobile phase to obtain a yellow liquid (45 mg, 82%). ^{1}H NMR ($CDCl_3$, 400 MHz): δ 11.37 (bs, NH), 6.30 (t, *J* = 7.2 Hz, $N\underline{H}$-CH_2-CH_2-CH_3), 4.34 (q, *J* = 7.2 $COOC\underline{H}_2CH_3$), 3.22 (q, *J* = 7.2 Hz, NH-$C\underline{H}_2$-CH_2-CH_3) 2.57 (br, 2H, H-8), 2.34 (br, 2H, H-5), 1.73 (m, 4H, H-6 y H-7), 1.61 (sext, *J* = 7.2 Hz, NH-CH_2-$C\underline{H}_2$-CH_3) 1.37 (t, *J* = 7.2 Hz, $COOCH_2C\underline{H}_3$), 0.96 (t, *J* = 7.2 Hz, NH-CH_2-CH_2-$C\underline{H}_3$). ^{13}C NMR ($CDCl_3$, 100 MHz): δ 169.4, 162.7, 158.0, 144.6, 104.7, 97.7, 60.7, 47.4, 27.2, 23.8, 23.6, 22.7, 21.1, 14.2, 11.3. EIMS *m/z* (Rel. Ab): $[M]^+$ 278 (43), 249 (20), 231 (35), 204 (60), 203 (100), 192 (40) uma.

2.2.14. Ethyl 4-(hexylamino)-2-oxo-1,2,5,6,7,8-hexahydroquinoline-3-carboxylate (8f)

In a round bottom flask, compound *7* (50 mg, 0.196 mmol) and ethanol (15 mL) were added. Once stirring started, hexylamine (0.10 mL, 0.784 mmol) was added drop by drop. The mixture was stirred for 48 h at reflux. Once the heating was completed, the mixture was cooled and concentrated in a rotary evaporator. Subsequently, the compound was purified by column chromatography with a mobile phase of ethyl acetate to obtain a yellow liquid (46 mg, 73%). ^{1}H NMR ($CDCl_3$, 400 MHz): δ 11.20 (bs, NH), 6.23 (bs, $N\underline{H}$-CH_2-CH_2-$(CH_2)_3$-CH_3), 4.34 (q, *J* = 7.2 $COOC\underline{H}_2CH_3$), 3.24 (q, *J* = 7.2 Hz, NH-$C\underline{H}_2$-CH_2-$(CH_2)_3$-CH_3), 2.56 (br, 2H, H-8), 2.33 (br, 2H, H-5), 1.73 (m, 4H, H-6 y H-7), 1.58 (quint, *J* = 7.2 Hz, $NHCH_2$-$C\underline{H}_2$-$(CH_2)_3$-CH_3) 1.37 (t, *J* = 7.2 Hz, $COOCH_2C\underline{H}_3$), 1.30 (m, 6H, NH-CH_2-CH_2-$(C\underline{H}_2)_3$-CH_3) 0.96 (t, *J* = 7.2 Hz, NH-CH_2-CH_2-$(CH_2)_3$-$C\underline{H}_3$). ^{13}C NMR ($CDCl_3$, 100 MHz): δ 169.4, 162.6, 157.9, 144.5, 104.6, 97.8, 60.7, 45.7, 31.4, 30.5, 27.2, 26.5, 23.6, 22.7, 22.5, 21.2, 14.3, 13.9. EIMS *m/z* (Rel. Ab): $[M]^+$ 320 (36), 273 (27), 247 (26), 217 (30), 203 (100) uma.

2.2.15. Ethyl 2-oxo-4-(prop-2-yn-1-ylamino)-1,2,5,6,7,8-hexahydroquinoline-3-carbo-xylate (8g)

In a round bottom flask, compound *7* (50 mg, 0.196 mmol) and ethanol (15 mL) were added. Once stirring started, propargylamine (0.05 mL, 0.784 mmol) was added drop by drop. The mixture was stirred for 48 h at reflux. Once the heating was completed, the mixture was cooled and concentrated in a rotary evaporator. Subsequently, the compound was purified by column chromatography with an ethyl acetate mobile phase to obtain a yellow liquid (43 mg, 80%). ^{1}H NMR ($CDCl_3$, 400 MHz): δ 11.49 (bs, NH) 6.63 (t, *J* = 5.2 Hz, $N\underline{H}$-CH_2), 4.36 (q, *J* = 7.2 Hz, $COOC\underline{H}_2CH_3$), 4.02 (dd, *J* = 5.2 Hz, 2.4 Hz, $NHC\underline{H}_2$) 2.60 (br, 2H, H-8), 2.40 (br, 2H, H-5), 2.32 (t, *J* = 2.4 Hz, C≡C$\underline{H}$) 1.75 (m, 4H, H-6 y H-7), 1.37 (t, *J* = 7.2 Hz, $COOCH_2C\underline{H}_3$). ^{13}C NMR ($CDCl_3$, 100 MHz): δ 169.0, 162.6, 157.9, 145.6, 105.3, 99.4, 80.1, 72.9, 60.9, 35.4, 27.1, 23.5, 22.6, 21.1, 14.2. EIMS *m/z* (Rel. Ab): $[M]^+$ 274 (27), 245 (29), 227 (29), 205 (100), 203 (99) uma.

2.3. HIV-1 RT inhibition assays

Reverse transcriptase enzyme inhibition assays were performed in 96-well cell culture dishes using the EnzChek® Reverse Transcriptase Assay kit (invitrogen, USA) according to the user manual. In a microtube, the dT and poly A18 oligos were aligned for 1 h, 10 µl of the mixture of aligned oligonucleotides was placed in each well, then the compounds were added at concentrations of 0.01, 0.05, 0.1, 4, 40 and 100 µM to subsequently add 0.625 units of a recombinant reverse transcriptase enzyme (Merck, Germany) diluted in enzyme diluent buffer (50mM Tris-HCl (pH 8.3, 25°C), 75mM KCl, 3mM $MgCl_2$ and 10mM DTT). The experimental design included a negative control that contains all the elements necessary for the reaction except the reverse transcriptase and a positive control that contains all the components without any drug and an inhibition control with reference drugs (Efavirenz, Nevirapine); The reaction was carried out

for 45 minutes and was stopped by adding 200 mM EDTA. Subsequently, 173 µL of picogreen solution was added to the well, which is a dye that is specifically intercalated with the RNA-DNA or DNA hetero-duplex, which was incubated for 5 minutes at room temperature. The absorbance measurement was performed in a spectrophotometer. (BioTek, USA), the samples were excited at 485 nm and the measurement was performed at 520 nm.

2.4. Antiviral activity assay

Viral replication inhibition assays were carried out by seeding JLTRG cells in duplicate in 96-well cell culture dishes at a density of 50,000 cells/well, the compounds were added at concentrations of 0.01, 0.05, 0.1, 4, 40 and 100 µM and co-incubated for 1 h. Subsequently, the supernatant with virus suspended in 1X RPMI medium with 10% fetal bovine serum was added to obtain a concentration necessary to obtain an MOI of 0.1; The cultures were kept in incubation with the compounds and the virus at 37°C, 5% CO_2 and 95% atmospheric air for 48 h.

The samples were collected in microtubes where they were fixed with 2% paraformaldehyde for 30 minutes at 4°C, then two washes with 1X PBS were performed. The percentage of fluorescent cells that express the EGFP protein was measured by flow cytometry using the Attune Blue/Violet cytometer (Thermo Fisher, USA) using the blue laser (488 nm), the EGFP protein emits at 520 nm, using The BL1 detector detected the percentage of EGFP-positive cells. The determination of EC_{50} was carried out in the Graphpad Prism version 6.0 program. A non-linear regression was carried out on the data obtained by creating a dose response curve for each compound. The data were normalized with respect to the control group: HIV-1 infected cells without treatment for in vitro infection.

2.5. Cytotoxicity evaluation

To measure cytotoxicity, the CellTiter 96® Non-Radioactive Cell Proliferation Assay kit from Promega (Madison, USA) was used in JLTRG cells quantifying the color change of 3-(4,5-dimethylthiozol-2-yl)-bromide. of 2,5-diphenyltetrazole (MTT), in the presence of different concentrations of the synthesized compounds (0.01, 0.05, 0.1, 4, 40 and 100 µM). According to the procedure, JLTRG cells were seeded in the 96-well plate at a density of 50,000 cells/well and incubated at 37 °C in a 5% CO_2 incubator for 48 h. The incubated cells were treated with different concentrations of the compounds. After treatment, 20 µl of dissolved MTT at 5 mg/ml was added to each well and incubated for another 4 h. After incubation, the formed MTT-formazan crystals were dissolved in stopping solution (0.01N Tris HCL, 10% SDS) by adding 100 µl to each well. Finally, the plate was incubated in darkness for 5 min and the color change and absorbance were recorded at 570 nm using the iMarck plate reader from Bio-Rad (USA). The experiments were performed in triplicate. The determination of CC_{50} was carried out in the Graphpad Prism version 6.0 program. A non-linear regression was carried out on the data obtained by creating a dose response curve for each compound. The data were normalized with respect to the control group: cells without treatment for the MTT assay.

2.6. *In silico* prediction of pharmacokinetic parameters

All the selected molecules were analyzed for the prediction of their pharmacokinetic parameters related to absorption, distribution, metabolism and excretion (ADME) using the SwissADME server [15], and evaluated using Lipinski's rule of five for drug-likeness.

2.7. Molecular docking studies

The three-dimensional structures of the two receptors, HIV-1 reverse transcriptase and reverse transcriptase with the Y188L mutation were retrieved from the Protein Data Bank (http://www.rcsb.orq/pdb/home/home.do) using PDB IDs: 2BE2 [16] and 1BQN [17], respectively. The receptors were prepared for molecular docking using Chimera software [18], where the water molecules, ions and other co-crystallized ligands present were removed using the protein preparation module present in the program. The synthesized compounds Molecular docking studies of the created compounds were carried out with the use of the program Autodock VINA [19, 20]. Through Autodock Vina and its graphical interface AutoDockTooIs 1.54 (ADT) non-polar hydrogens were eliminated and Gasteiger-MarsiIi charges were added. With the ADT program, using the AutoGrid 4.2 auxiliary program, the search box or grid was generated, which was positioned in the place of the co-crystallized ligand of the RT enzyme. The search for conformations accessible by the ligands was performed using AutoDock Vina with an exhaustiveness of 32 runs. Finally, the best docking models were selected, and two-dimensional docking maps created, which were designed using the Poseview server [21, 22] and the Discovery Studio Visualizer program [23]. The molecular docking protocol was validated by re-docking the co-crystallized ligand of the RT enzyme and evaluating of the RMSD value of its highest-ranking docked pose. The docking pose had a RMSD value of 1.001 Å.

2.8. Molecular dynamics

The ligand-protein complex of compound *8e* with the RT enzyme obtained from molecular docking was subjected to MD simulation. The study was performed using GROMACS, version 2023.3 [24]. The complex was subjected to 100 ns dynamic simulation in an explicit water model using the CHARMM27 force field [25]. To represent water molecules, the TIP3P model was used [26]. The compound 8e topology file was created via SwissParam Server [27]. To mimic physiological conditions, 0.15 M salt (NaCl) was added. Before running production, the system was equilibrated by running 100 ps of NVT ensemble (isothermal -isochoric) and NPT (isothermal-isobaric). The simulation system was closely monitored to reach a temperature of 300 K and around 1 atmospheric pressure. MD simulations were then carried out in a triclinic box with a minimum distance of 1.0 nm between any atom of the protein and the walls of the box. The root mean square deviation (RMSD) of protein, root mean square fluctuation (RMSF) of amino acid residues, radius of gyration (rg), and hydrogen bonds were plotted using XMGRACE v5.1.19 [28].

3. Results and Discussion

3.1. . Chemistry

Pyridinone derivatives were synthesized using the methodology described in Scheme 1. All compounds were synthesized from the common intermediate *3*, which was conveniently prepared by condensation of ethyl 2-oxocyclohexanecarboxylate *(1)* with commercially available diethyl malonate [29]. In obtaining *6a-d* the *o*-benzylation of *3* was first necessary to obtain *4*, which easily underwent the Williamson reaction [30] with the corresponding alkyl bromide to give *5a-d*. The series of benzyl-protected esters were heated in aqueous HCl in order to debenzilate and provide *6a-d*. The compound *6b* is a pyridinone-UC781 hybrid. For the preparation of the amino analogues *8e-g*, the pyridinone nucleus *3* was chlorinated with phosphorus oxychloride and benzyltriethylammonium chloride to obtain *7*, finally substituting it in the C-4 position with different amines [29]. All substituted compounds were further purified by washing, recrystallized and then characterized by NMR, IR and MS. The performance of the molecules is reported with spectral data.

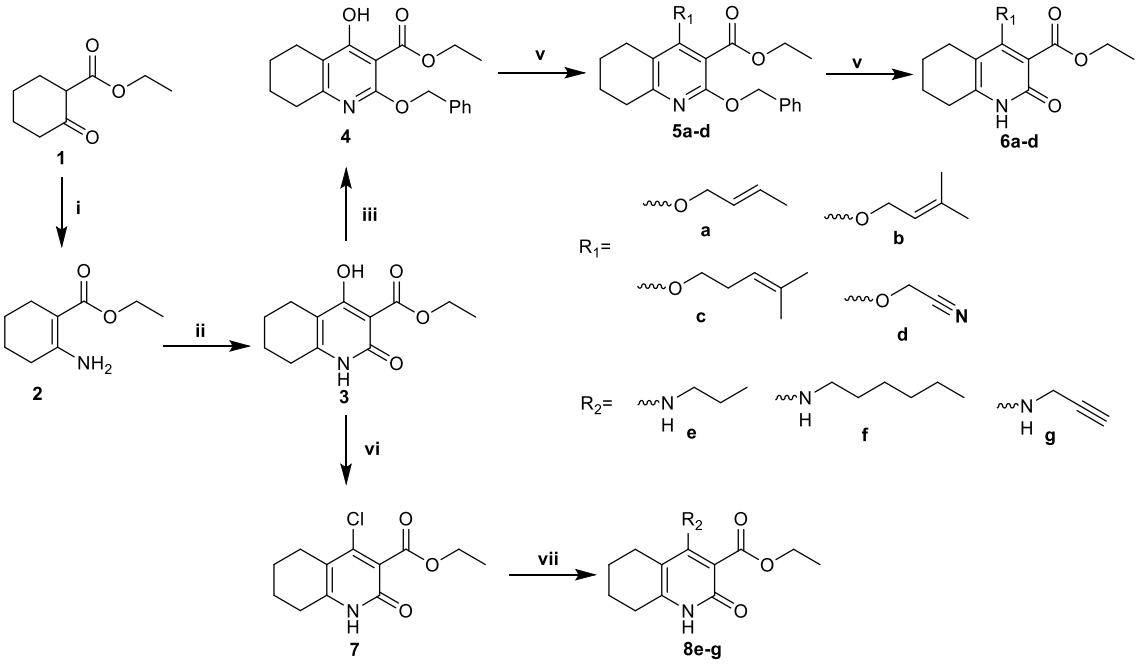

Scheme 1 Synthesis of cyclohexanpyridinone derivatives[a]

[a]Reagents conditions: (i) NH_4NO_3, THF anhydride, NH_3, *5d*; (ii) diethyl malonate /EtONa/EtOH/ reflux; (iii) $PhCH_2Br$, Ag_2CO_3, THF, reflux, 8 h; (iv) alkyl bromide, K_2CO_3, DMF, rt, 72 h; (v) HCl 0.75 N, rt, 48 h; (vi) $POCl_3$, benzyltriethylammonium chloride/CH_3CN/rt, 12h (vii) amine/EtOH/reflux, 48 h.

3.2. Pharmacokinetic parameters

Molecular weight (MW), octanol/water partition coefficient (log P), topological polar surface area (tPSA), water solubility (log Sw), hydrogen bond acceptors (HBA), hydrogen bond donors (HBD), solubility (mg/ mL) and number of rotatable bonds were calculated for the final synthesized compounds using the SwissADME server. Almost all the compounds showed good pharmacokinetic parameters and drug-like properties as contrived by Lipinski's rule of five (Table 1).

Table 1 Predicted properties of the compounds selected for docking studies.

Compound	MW	Rotatable bonds	HBA	HBD	TPSA	Log P	Log S	Solubility (mg/mL)
5a	381.46	9	5	0	57.65	4.58	-5.05	3.43E-03
6a	291.34	6	4	1	68.39	2.67	-2.69	5.95E-01
6b	305.37	6	4	1	68.39	3.09	-3.16	2.09E-01
6d	276.29	5	5	1	92.18	1.59	-1.99	2.81E+00
6c	319.4	7	4	1	68.39	3.33	-3.47	1.09E-01
8e	278.35	6	3	2	71.19	2.59	-2.99	2.84E-01
8f	320.43	9	3	2	71.19	3.61	-3.93	3.74E-02
8g	274.32	5	3	2	71.19	2.23	-2.54	7.88E-01

3.3. Molecular docking

This study aimed to provide a union model between the compounds and the 3D structure of the RT enzyme. Docking simulations were performed by energy minimization and optimization of the synthesized compounds at the binding site of the crystallized reverse transcriptase enzyme using PDB ID: 2BE2. This 3D structure was chosen due to the structural similarity of the co-crystallized ligand with the synthesized pyridinones. The compounds docked at the allosteric site of the enzyme producing a similar binding pattern and positioning as the co-crystallized ligand R221239 (Figure 2). In addition, the docking of the compounds efavirenz and nevirapine was carried out to compare the results with these currently used drugs. The docking score (binding free energy, ΔG°, kcal/mol) of the designed pyridinones with the enzyme are summarized in Table 2

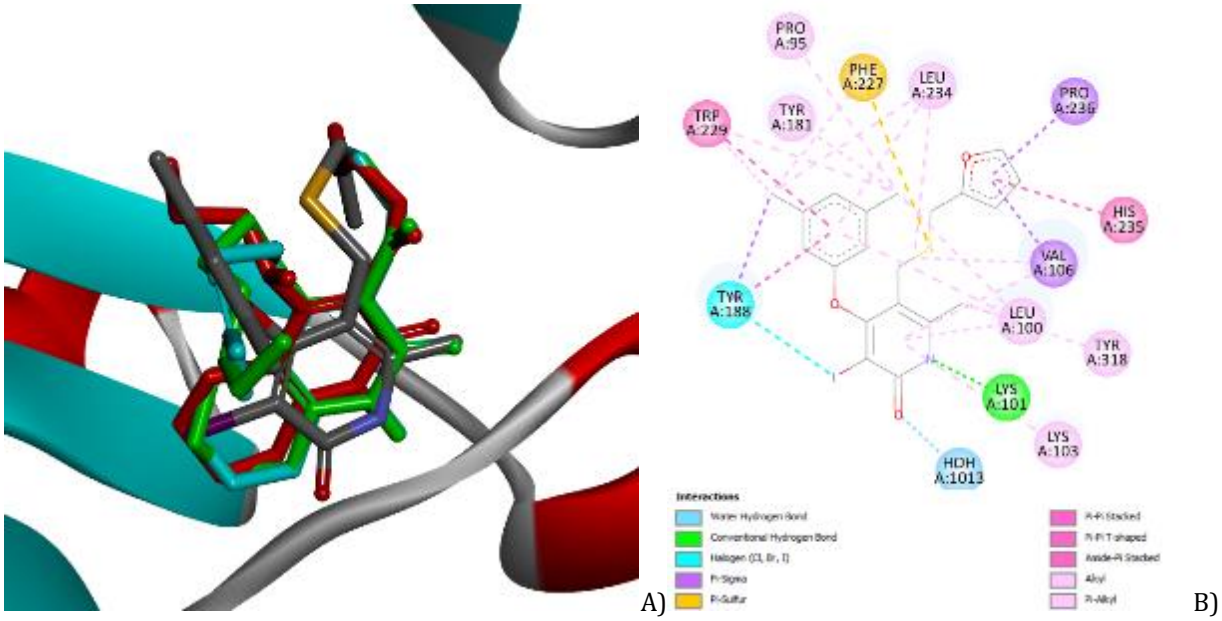

Figure 2 A) Superimpose of *8e* (blue), *8f* (green) and *8g* (red) with co-crystallized ligand of 2BE2 (grey) in the binding site of RT; B) Interactions of the co-crystallized ligand R221239 with the RT enzyme.

Table 2 Docking scores of compounds with RT

	Vina
Compound	**Score (ΔG, kcal / mol)**
5a	-8.0
6a	-8.5
6b	-9.6
6c	-9.0
6d	-7.5
8e	-8.5
8f	-8.7
8g	-8.5
Efavirenz	-11.4
Nevirapine	-7.4
R221239	-11.6

The molecular docking analysis of the synthesized pyridinones against RT highlighted compounds *6a*, *6b*, *6c*, *8e*, *8f* and *8g* with the most favorable docking values. The overlap of the docked poses of these ligands at the site of binding showed that they have a binding pattern and orientation similar to that of the co-crystallized ligand.

As shown in Figure 3, the interactions presented by compounds *6a*, *6b* and *6c*, which contain alkenyloxy groups in R_1, highlight the hydrogen bond with Lys101. This interaction is of vital importance for the anchoring of the compounds in the allosteric site of the RT [31]. On the other hand, interaction with Tyr188, an important interaction performed by the R221239 co-crystallized ligand, also stands out for the compounds.

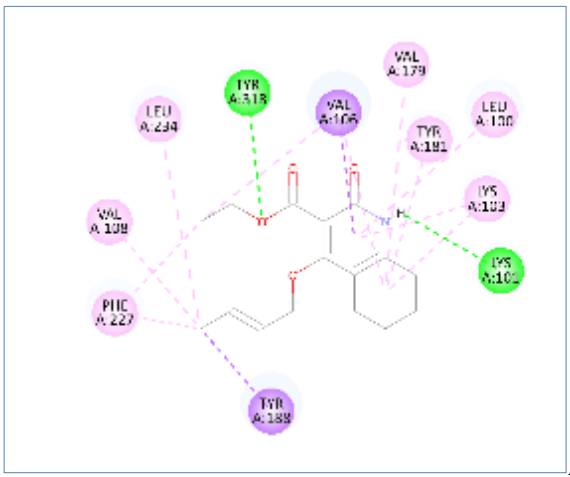

A)

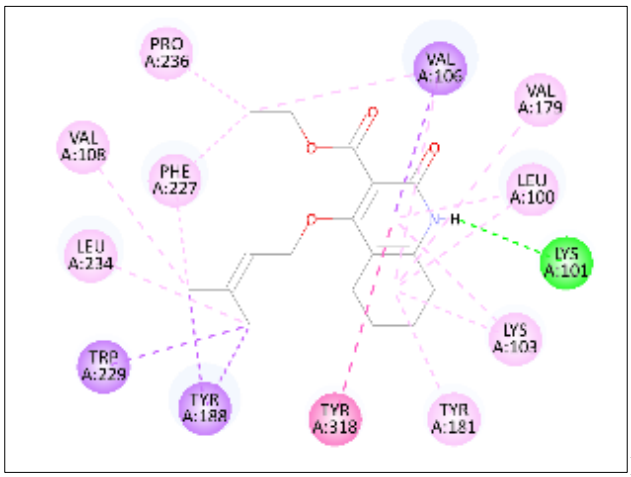

B)

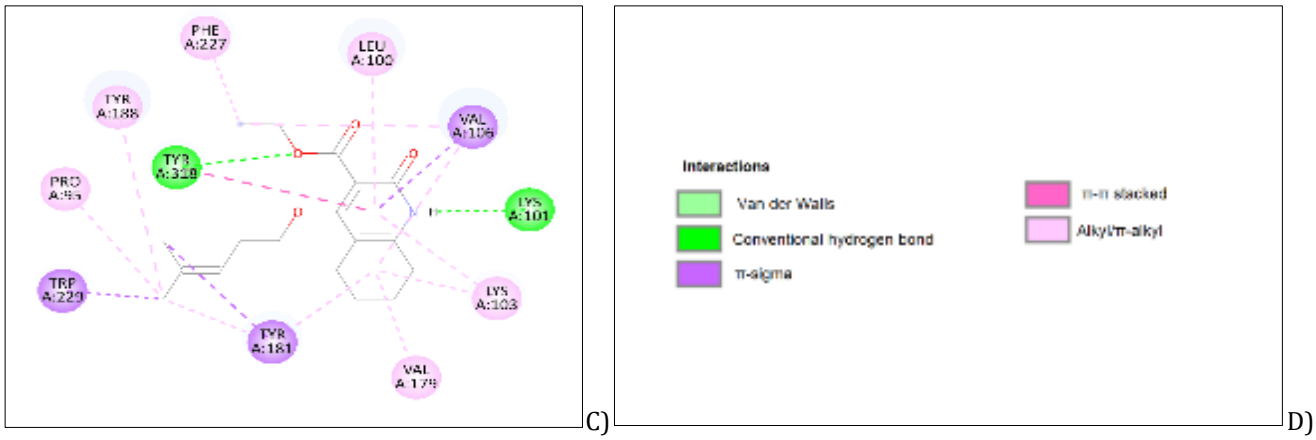

Figure 3 Two-dimensional maps of the predicted interactions of the new pyridinones with RT. A) *6a*, B) *6b*, C) *6c*.

The analysis of the predicted binding modes of compounds *8e*, *8f* and *8g*, which contain amino groups in R_1, with RT first showed that they were capable of generating hydrogen bond interactions with Lys101. Furthermore, the substituents on R_1 showed interactions with Tyr188, similar to the R221239 co-crystallized ligand (Figure 4).

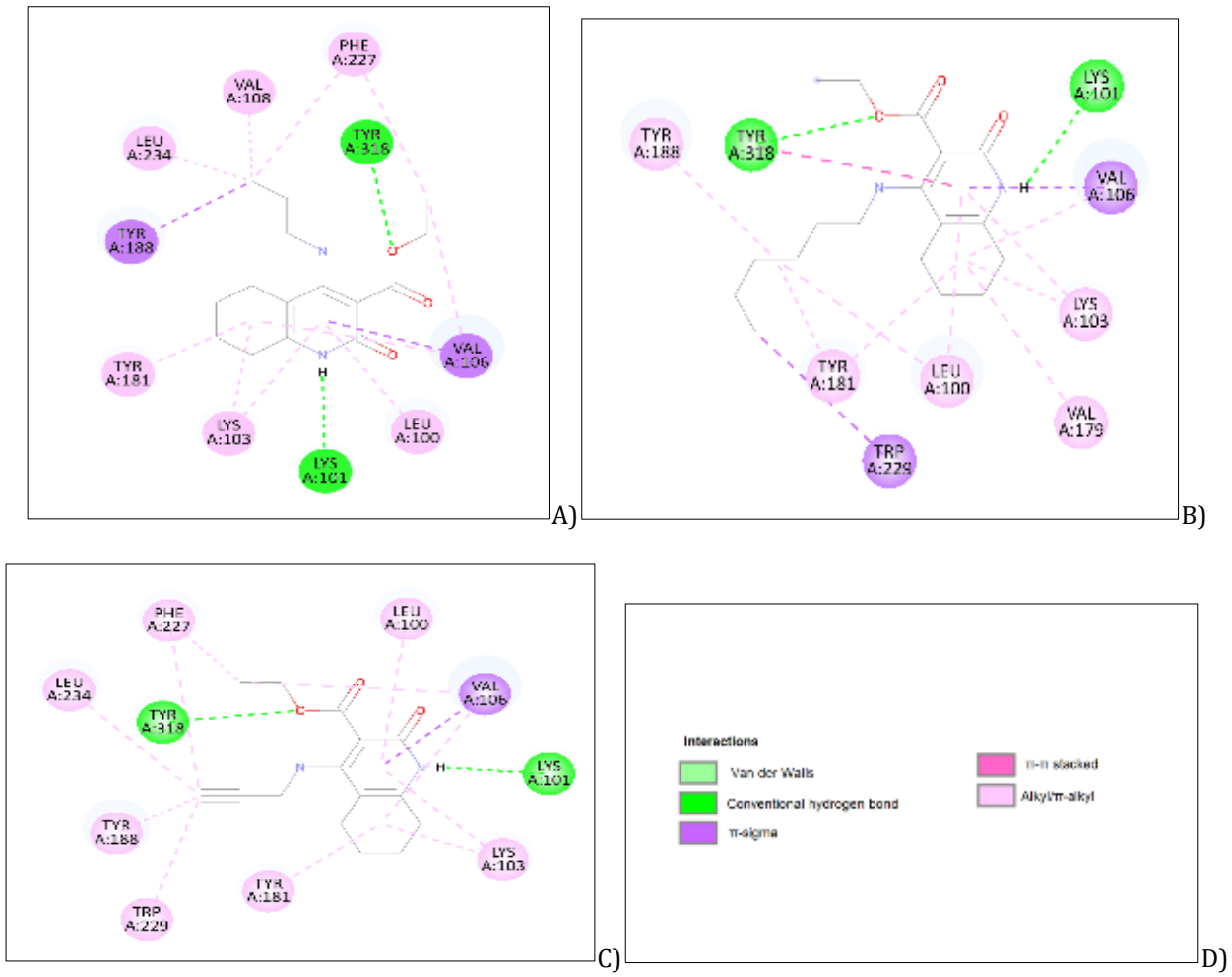

Figure 4 Two-dimensional maps of interactions with RT. A) *8e*, B) *8f*, C) *8g*.

Additionally, the molecular docking of the compounds was carried out with the crystal structure of the RT which contains the Y188L mutation (PDB ID: 1BQN). This was done to analyze the interactions of the compounds in the face of such a mutation and observe the flexibility of the substituents to establish interactions in the allosteric site of the enzyme. The docking results of the eight synthesized compounds, as well as the compounds efavirenz and nevirapine,

are shown in Table 3. The analysis of the compounds was carried out by comparing the docking poses obtained superimposed to the co-crystallized ligand HBY 097 (Figure 5).

Table 3 Energy score of the compounds against mutant RT.

	Vina
Compounds	**Score (ΔG, kcal / mol)**
5a	-9.7
6a	-8.4
6b	-9.0
6c	-8.8
6d	-7.6
8e	-8.0
8f	-8.8
8g	-8.1
Efavirenz	-9.4
Nevirapine	-8.9
HBY 097	-7.7

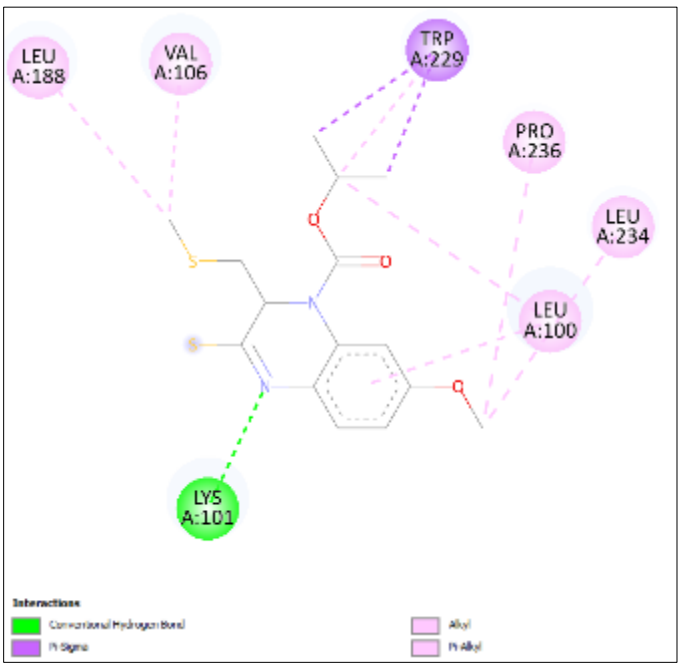

Figure 5 Interactions of the HBY 097 co-crystallized ligand in the mutant RT enzyme**.**

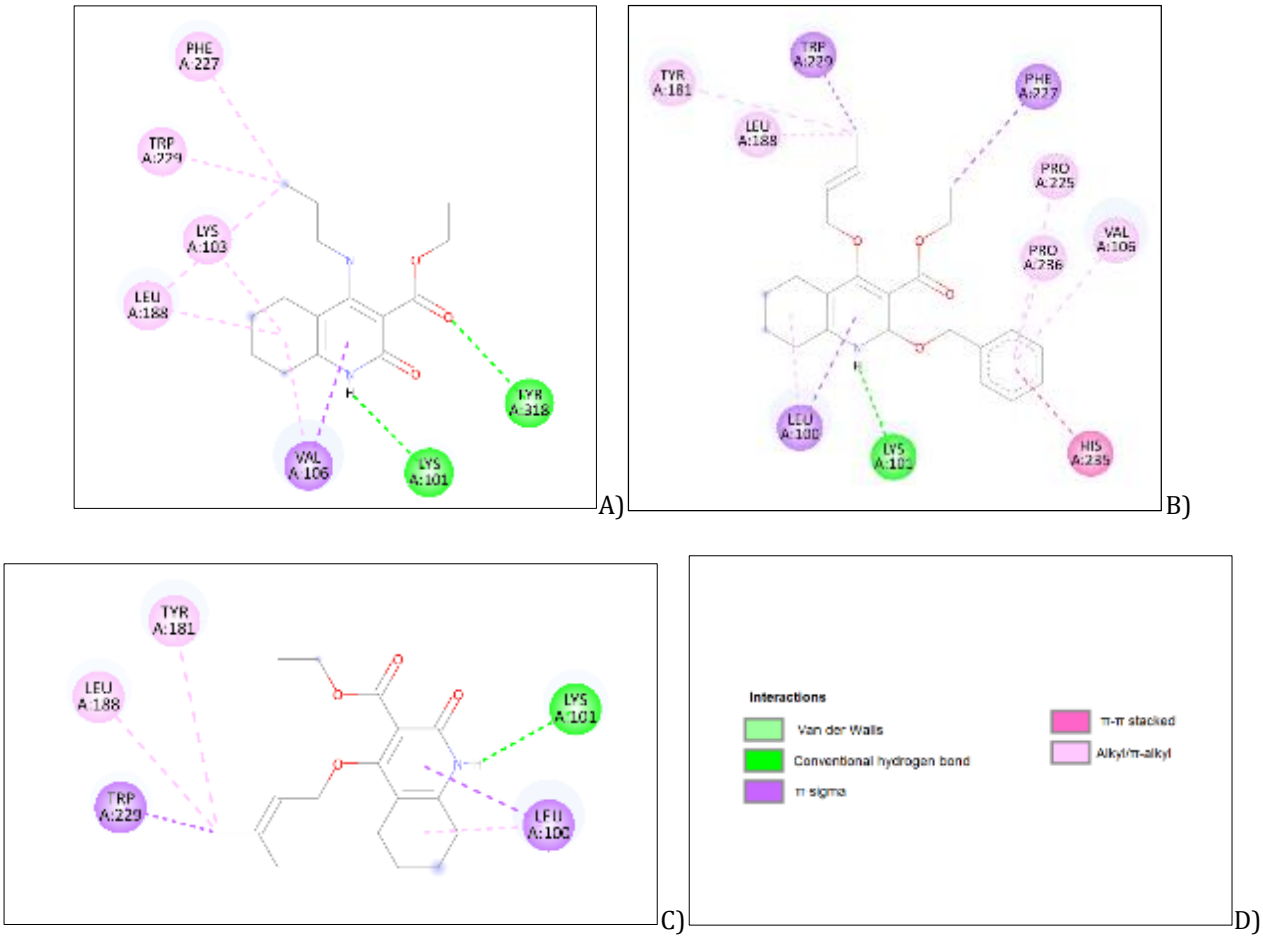

Figure 6 Two-dimensional maps of interactions with the Y188L mutant RT enzime. A) *8e*, B) *6b*, C) *5a*

According to the predicted binding modes, the compounds make the key hydrogen bond interaction with Lys101 (Figure 6). Furthermore, in the Y188L mutation, the substituents in the C-4 position of the compounds were able to establish interactions with the Leu188 residue. Even the flexibility of the substituents allows them to interact with the Tyr181 residue (Figure 6).

3.4. Biological evaluation

3.4.1. Cellular cytotoxicity (MTT) of cyclohexanpyridinone derivatives

The cytotoxicity of cyclohexanpyridinone derivatives was evaluated by the percentage of viability using the MTT assay [32, 33] in Olaf Kutsch's Jurkat LTR-GFP (JLTRG) cells donated by the NIH AIDS Reagent Program (EU). These are derived from the cell line Jurkat (immortalized T lymphocytes obtained from a patient with leukemia) [34] per well in the presence of increasing concentrations of the compounds (0.01-100 µM).

The results of the analysis of the 50% cellular cytotoxic concentration (CC_{50}) showed that the molecules that have the amino substituent at C-4 *8e* and *8g* have a CC_{50} >100 µM, therefore, they are not cytotoxic at the concentrations evaluated. Compound *8e* showed the dose response curve in Figure 8A. The compound was not cytotoxic at the concentrations evaluated, being less cytotoxic than efavirenz and nevirapine, which were the drugs used as controls. It is worth noting that derivative *8f* showed to be highly cytotoxic (CC_{50} = 0-21 µM). These differences in citotoxicity seem to be related to the chain length of the C-4 substituent, since *8e* and *8g* have a three-carbon chain while *8f* has a six-carbon chain (Scheme 1).

Derivatives with an alkenyloxy substituent at C-4 *6c* and *6d* were not citotoxic at the concentrations used, with CC_{50} > 100 µM, while *6a* and *6b* were shown to be moderately cytotoxic (CC_{50} = 69 and 35 µM, respectively). Compound *5a* showed moderate cytotoxicity (CC_{50} = 60 µM). Thus, the benzyl substituent in the C-2 position of compound *5a* did not show to decrease cytotoxicity.

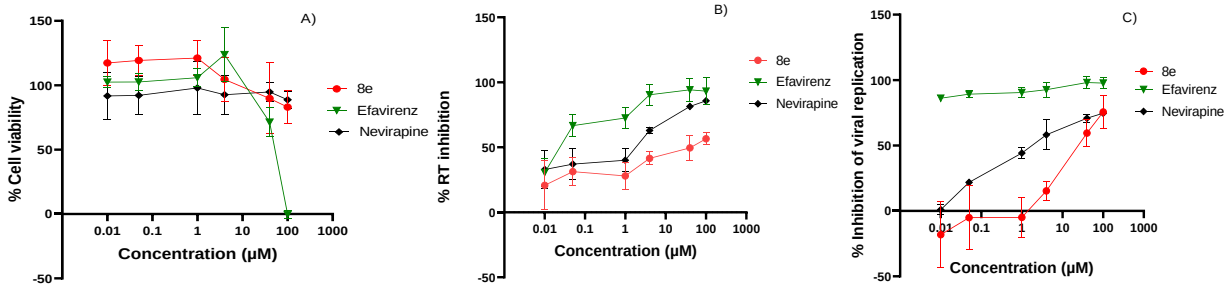

Figure 8 Dose-response curve. A) Percentage of cell viability; B) Percentage of inhibition of TI; C) Percentage of viral replication inhibition of compound 8e versus efavirenz and nevirapine.

3.4.2. Reverse transcriptase inhibition assay

Inhibition of the compounds against RT was performed with the CellTiter 96® Non-Radioactive Cell Proliferation Assay kit from Promega (Madison, USA), as described by the manufacturer. The inhibitory concentration 50 (IC_{50}) was determined using the same increasing concentrations and culture conditions as the cytotoxicity assay. Efavirenz and nevirapine were used as positive controls. Evaluation of the inhibition of the compounds showed that cyclohexanpyridinone derivatives moderately inhibit reverse transcriptase activity and virus replication with inhibition percentages of 23 to 56% against RT activity. *5a* showed inhibitory activity against RT of 23%, while compound *6a* inhibited the enzyme in a concentration-dependent manner until reaching 40% inhibition at 100 μM, demonstrating the importance of the NH hydrogen of the pyridinone nucleus. Compound *8e* also stands out (Figure 8B), with an IC_{50} value of 69.8 μM, thus showing the best inhibition. The rest of the compounds showed no reverse transcriptase inhibitory activity at the concentrations tested, so the IC50 values, if any, were >100 μM.

3.4.3. Anti-HIV and anti-RT activity of compounds

Table 4 Inhibition of RT activity, anti-HIV activity and cytotoxicity of cyclohexanpyridinone derivatives compared to efavirenz and nevirapine.

Compound	Substituent at C-4	CC_{50} (μM)[a]	RT IC_{50} (μM)[b]	HIV EC_{50} (μM)[c]
5a	Crotyl	60.0	>100	>100
6a	Crotyl	69.0	>100	71.4
6b	Isopentenyl	35.0	>100	>100
6c	Isohexenyl	>100	>100	>100
6d	Cyanomethyl	>100	>100	>100
8e	Propyl	>100	69.8	28.8
8f	Hexyl	0.02	>100	>3.9
8g	Propargyl	>100	>100	>100
Nevirapine		>100	3.71	0.4217
Efavirenz		42.94	0.014	0.0046

[a]CC_{50} =Concentration required to reduce the viability of cell cultures by 50%, as determined by the MTT method; [b]IC_{50} = Concentration required to inhibit by 50% the in vitro of RT activity; [c]EC_{50} = Concentration required to inhibit HIV viral infectivity by 50%.

All cyclohexanpyridinone derivatives were evaluated in an *in vitro* infection model. The JLTRG reporter cell line infected by HIV-1 (strain IIIB) was used [34, 35, 36]. The IC_{50} values for the cyclohexanpyridinone derivatives are shown in Table 4. Results showed that compounds *5a* and *6b* were cytotoxic at concentrations <100 μM and did not showed capacity to inhibit HIV infectivity. Compound *6a*, which seemed to inhibit virus replication (IC_{50} = 71.4 μM), had a CC_{50} of approximately the same concentration (69 μM), so that virus inhibition may be due to the induction of cell damage by the compound and not to a specific antiviral effect. Notably, compound *8e* had an IC_{50} of 28.78 μM in the viral infectivity inhibition assay. In the dose-response curve (Figure 8C), it was observed that both nevirapine and compound *8e*

inhibited the 75% of viral replication at the same concentration (100 μM). Importantly, as shown before, *8e* showed low cytotoxicity (CC_{50} > 100 μM), an inhibited the activity of the RT (IC_{50} = 69.8 μM) (Figure 8B and Table 4).

3.5. Molecular dynamics simulation

Based on the results of the docking and biological tests, a MD simulation was carried out to predict the interactions and stability of compound *8e* upon binding to the allosteric site of the RT.

The RMSD analysis indicates whether the simulation has equilibrated or not. Figure 9a shows the RMSD of the ligand when the protein-ligand complex is first aligned on the protein backbone of the reference molecule and then the RMSD of the ligand heavy atoms is measured. RMSD changes of the order of 0.1-0.3 nm are perfectly acceptable for small proteins, while much larger changes indicate that the protein is undergoing a large conformational change during the simulation [37]. In this study, the complex of *8e* with RT was simulated for 100 ns. In Figure 9A it is observed that there was a small fluctuation in the RMSD value of the complex up to 10 ns, and then it converged and remained stable at 0.3 nm during the 100 ns duration of the MD simulation, which indicated that the complex of compound *8e* with RT stabilized after 10 ns.

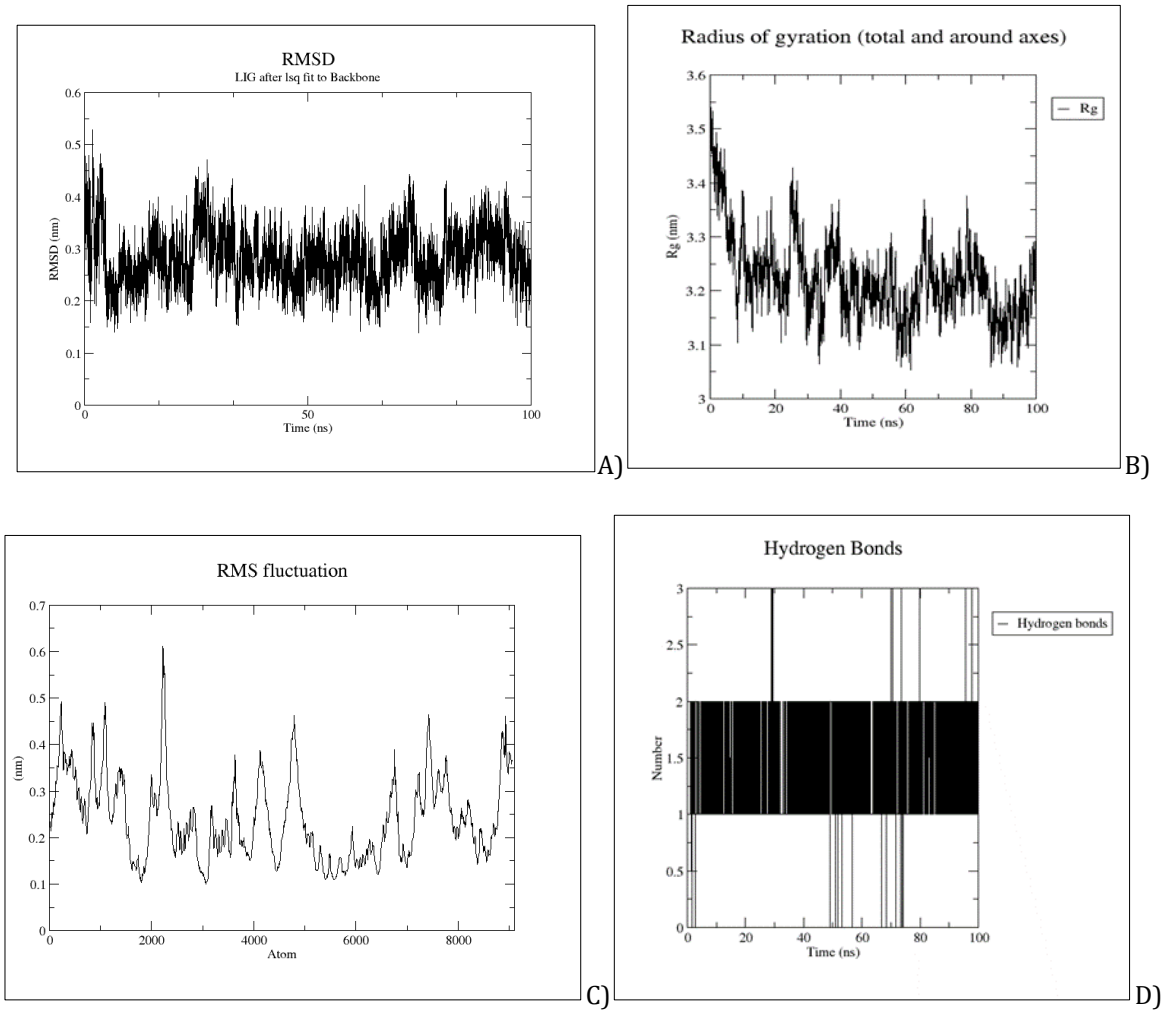

Figure 9 Stabilities of *8e* in complex with RT during 100 ns MD simulation. A) RMSD values of the RT:*8e* protein backbone complex. B) Rg (radius of gyration) of the RT:*8e* complex as a function of time. C) RMSF values of amino acids of the RT:*8e* complex. D) Number of intermolecular H bonds between *8e* and RT**.**

The RMSF is an indicator of flexibility and shows local changes in protein structure. Since RMSF measures the deviations of the residue from its initial position, it is also very useful for exploring the conformational flexibility of protein-ligand complexes. As seen in Figure 9C, the compound maintained close contact with its binding site during the MD simulations.

The number of intermolecular hydrogen bonds is an important parameter that can be used to quantify the binding affinity between the protein and the ligand molecule. The presence of a large number of hydrogen bonds between the protein and the ligand means a strong bond between the molecules. Two hydrogen bonds were generally established in the complex during the 100 ns of simulation (Figure 9D).

4. Conclusions

With the aim of finding new HIV RT inhibitors containing a 2-pyridinone structure, pyridinone derivatives (*5a*, *6a-d*) and other compounds with alkylated amino groups at the C-4 position (*8e-g*) were synthesized. A molecular docking analysis was performed showing that the pyridinone derivatives have a binding pattern and orientation similar to that of the co-crystallized ligand, in addition to similar scores to the drugs used as controls in the biological tests. Docking analysis also showed the potential of compounds to bind the Y188L mutant enzime. Compound *8e* showed moderate *in vitro* enzymatic inhibitory activity toward wild-type HIV RT, good activity against HIV strain IIIB, and is not cytotoxic for the human lymphocytic JLTRG cell line; therefore, it is the compound that had the best activity profile and can be classified as NNRTIs. In the MD results, *8e* established two hydrogen bonds and good stability in the 100 ns of simulation, indicating a good affinity to the RT enzyme. Furthermore, *8e* docking with a mutant RT enzyme showed flexibility of substituents to establish interactions at the allosteric site. This study stands out the relevance of the continuous search of synthetic small compounds against the HIV reverse transcriptase and their *in vitro* evaluation. Considering the findings of this study regarding the structural requirements and biological activity profiles of the tested compounds, further development of amino-type pyridinone-derived compounds similar to *8e* (hit compound) will likely provide novel and more potent RT inhibitors for the treatment of HIV.

Compliance with ethical standards

Acknowledgments

We thank Consejo Nacional de Ciencia y Tecnología CONACyT, Grant 155029 to DC, and Dirección General de Asuntos del Personal Académico of Universidad Nacional Autónoma de México, Grant PAPIIT AG200623 to LH. GR-V acknowledges support from CONAHCyT in the form of graduate scholarship. We thank CONAHCyT for ITT NMR facilities (Grant INFR-2011-3-173395).

Disclosure of Conflict of interest

No conflict of interest to be disclosed.

References

[1] HIV, U. G. (2023). AIDS statistics-2022 fact sheet. *Geneva: UNAIDS*.

[2] Brechtl JR, Breitbart W, Galietta M, Krivo S, Rosenfeld B. The use of highly active antiretroviral therapy (HAART) in patients with advanced HIV infection. J Pain Symptom Manage. 2001;21(1):41–51.

[3] Zhuang C, Pannecouque C, De Clercq E, Chen F. Development of non-nucleoside reverse transcriptase inhibitors (NNRTIs): our past twenty years. Acta Pharm Sin B. 2020;10(6):961–78.

[4] Cilento ME, Kirby KA, Sarafianos SG. Avoiding drug resistance in HIV reverse transcriptase. Chem Rev. 2021;121(6):3271–96.

[5] Broder S. The development of antiretroviral therapy and its impact on the HIV-1/AIDS pandemic. Antiviral Res. 2010;85(1):1–18.

[6] Wang Y, Wang X, Xiong Y, Kaushik AC, Muhammad J, Khan A, et al. New strategy for identifying potential natural HIV-1 non-nucleoside reverse transcriptase inhibitors against drug-resistance: an *in silico* study. J Biomol Struct Dyn. 2020;38(11):3327–41.

[7] de Béthune M-P. Non-nucleoside reverse transcriptase inhibitors (NNRTIs), their discovery, development, and use in the treatment of HIV-1 infection: A review of the last 20 years (1989–2009). Antiviral Res. 2010;85(1):75–90.

[8] Zhan P, Chen X, Li D, Fang Z, De Clercq E, Liu X. HIV-1 NNRTIs: structural diversity, pharmacophore similarity, and impliations for drug design. Med Res Rev. 2013;33(S1).

[9] Medina-Franco JL, Martínez-Mayorga K, Juárez-Gordiano C, Castillo R. Pyridin-2(1*H*)-ones: A promising class of HIV-1 non-nucleoside reverse transcriptase inhibitors. ChemMedChem. 2007;2(8):1141–7.

[10] Nunberg JH, Schleif WA, Boots EJ, O'Brien JA, Quintero JC, Hoffman JM, et al. Viral resistance to human immunodeficiency virus type 1-specific pyridinone reverse transcriptase inhibitors. J Virol. 1991;65(9):4887–92.

[11] Jorgensen WL, Ruiz-Caro J, Tirado-Rives J, Basavapathruni A, Anderson KS, Hamilton AD. Computer-aided design of non-nucleoside inhibitors of HIV-1 reverse transcriptase. Bioorg Med Chem Lett. 2006;16(3):663–7.

[12] Jorgensen WL. Computer-aided discovery of anti-HIV agents. Bioorg Med Chem. 2016;24(20):4768–78.

[13] Das K, Clark AD, Lewi PJ, Heeres J, de Jonge MR, Koymans LMH, et al. Roles of conformational and positional adaptability in structure-based design of TMC125-R165335 (etravirine) and related non-nucleoside reverse transcriptase inhibitors that are highly potent and effective against wild-type and drug-resistant HIV-1 variants. J Med Chem. 2004;47(10):2550–60.

[14] Medina-Franco JL, Rodríguez-Morales S, Juárez-Gordiano C, Hernández-Campos A, Jiménez-Barbero J, Castillo R. Flexible docking of pyridinone derivatives into the non-nucleoside inhibitor binding site of HIV-1 reverse transcriptase. Bioorg Med Chem. 2004;12(23):6085–95.

[15] Daina A, Michielin O, Zoete V. SwissADME: a free web tool to evaluate pharmacokinetics, drug-likeness and medicinal chemistry friendliness of small molecules. Sci Rep. 2017;7(1).

[16] Himmel DM, Das K, Clark AD, Hughes SH, Benjahad A, Oumouch S, et al. Crystal structures for HIV-1 reverse transcriptase in complexes with three pyridinone derivatives: A new class of non-nucleoside inhibitors effective against a broad range of drug-resistant strains. J Med Chem. 2005;48(24):7582–91.

[17] Hsiou Y, Das K, Ding J, Clark AD Jr, Kleim J-P, Rösner M, et al. Structures of Tyr188Leu mutant and wild-type HIV-1 reverse transcriptase complexed with the non-nucleoside inhibitor HBY 097: inhibitor flexibility is a useful design feature for reducing drug resistance. J Mol Biol. 1998;284(2):313–23.

[18] Pettersen EF, Goddard TD, Huang CC, Couch GS, Greenblatt DM, Meng EC, et al. UCSF Chimera—A visualization system for exploratory research and analysis. J Comput Chem. 2004;25(13):1605–12.

[19] Eberhardt J, Santos-Martins D, Tillack AF, Forli S. AutoDock Vina 1.2.0: New docking methods, expanded force field, and python bindings. J Chem Inf Model. 2021;61(8):3891–8.

[20] Trott O, Olson AJ. AutoDock Vina: Improving the speed and accuracy of docking with a new scoring function, efficient optimization, and multithreading. J Comput Chem. 2010;31(2):455–61.

[21] Stierand K, Maaß PC, Rarey M. Molecular complexes at a glance: automated generation of two-dimensional complex diagrams. Bioinformatics. 2006;22(14):1710–6.

[22] Fricker PC, Gastreich M, Rarey M. Automated drawing of structural molecular formulas under constraints. J Chem Inf Comput Sci. 2004;44(3):1065–78.

[23] Dassault Systèmes BIOVIA. Discovery Studio Modeling Environment, Release 2020. Dassault Systèmes; San Diego, CA, USA: 2020.

[24] Berendsen HJC, van der Spoel D, van Drunen R. GROMACS: A message-passing parallel molecular dynamics implementation. Comput Phys Commun. 1995;91(1–3):43–56.

[25] Vanommeslaeghe K, Hatcher E, Acharya C, Kundu S, Zhong S, Shim J, et al. CHARMM general force field: A force field for drug-like molecules compatible with the CHARMM all-atom additive biological force fields. J Comput Chem. 2010;31(4):671–90.

[26] Jorgensen WL, Chandrasekhar J, Madura JD, Impey RW, Klein ML. Comparison of simple potential functions for simulating liquid water. J Chem Phys. 1983;79(2):926–35.

[27] Zoete V, Cuendet MA, Grosdidier A, Michielin O. SwissParam: A fast force field generation tool for small organic molecules. J Comput Chem. 2011;32(11):2359–68.

[28] Turner, P. XMGRACE, Version 5.1. 19. Center for Coastal and Land-Margin Research, Oregon Graduate Institute of Science and Technology, Beaverton, OR (2005).

[29] Dolle V, Fan E, Nguyen CH, Aubertin A-M, Kirn A, Andreola ML, et al. A new series of pyridinone derivatives as potent non-nucleoside human immunodeficiency virus type 1 specific reverse transcriptase inhibitors. J Med Chem. 1995;38(23):4679–86.

[30] Le Van K, Cauvin C, de Walque S, Georges B, Boland S, Martinelli V, et al. New pyridinone derivatives as potent HIV-1 nonnucleoside reverse transcriptase inhibitors. J Med Chem. 2009;52(12):3636–43.

[31] Wang X, Zhang J, Huang Y, Wang R, Zhang L, Qiao K, et al. Design, synthesis, and biological evaluation of 1-[(2-benzyloxyl/alkoxyl)methyl]-5-halo-6-aryluracils as potent HIV-1 non-nucleoside reverse transcriptase inhibitors with an improved drug resistance profile. J Med Chem. 2012;55(5):2242–50.

[32] Mosmann T. Rapid colorimetric assay for cellular growth and survival: Application to proliferation and cytotoxicity assays. J Immunol Methods. 1983;65(1–2):55–63.

[33] Slater TF, Sawyer B, Sträuli U. Studies on succinate-tetrazolium reductase systems. Biochim Biophys Acta. 1963;77:383–93.

[34] Kutsch O, Levy DN, Bates PJ, Decker J, Kosloff BR, Shaw GM, et al. Bis-anthracycline antibiotics inhibit human immunodeficiency virus type 1 transcription. Antimicrob Agents Chemother. 2004;48(5):1652–63.

[35] Popovic M, Sarngadharan MG, Read E, Gallo RC. Detection, isolation, and continuous production of cytopathic retroviruses (HTLV-III) from patients with AIDS and pre-AIDS. Science. 1984;224(4648):497–500.

[36] Ratner L, Haseltine W, Patarca R, Livak KJ, Starcich B, Josephs SF, et al. Complete nucleotide sequence of the AIDS virus, HTLV-III. Nature. 1985;313(6000):277–84.

[37] Sangai NP, Patel CN, Pandya HA. Ameliorative effects of quercetin against bisphenol A-caused oxidative stress in human erythrocytes: an *in vitro* and *in silico* study. Toxicol Res (Camb). 2018;7(6):1091–9.